A face-selective ventral occipito-temporal map of the human brain with intracerebral potentials

Jacques Jonas[a,b,c,1], Corentin Jacques[a,1], Joan Liu-Shuang[a], Hélène Brissart[b], Sophie Colnat-Coulbois[d], Louis Maillard[b,c], and Bruno Rossion[a,2]

[a]Psychological Sciences Research Institute and Institute of Neuroscience, University of Louvain, B-1348 Louvain-La-Neuve, Belgium; [b]Neurology Unit, University Hospital of Nancy, F-54000 Nancy, France; [c]Centre de Recherche en Automatique de Nancy, UMR 7039, CNRS and University of Lorraine, F-54500 Vandœuvre-lès-Nancy, France; and [d]Neurosurgery Unit, University Hospital of Nancy, F-54000 Nancy, France

Edited by Aina Puce, Indiana University, Bloomington, IN, and accepted by Editorial Board Member Randolph Blake May 6, 2016 (received for review November 26, 2015)

Human neuroimaging studies have identified a network of distinct face-selective regions in the ventral occipito-temporal cortex (VOTC), with a right hemispheric dominance. To date, there is no evidence for this hemispheric and regional specialization with direct measures of brain activity. To address this gap in knowledge, we recorded local neurophysiological activity from 1,678 contact electrodes implanted in the VOTC of a large group of epileptic patients ($n = 28$). They were presented with natural images of objects at a rapid fixed rate (six images per second: 6 Hz), with faces interleaved as every fifth stimulus (i.e., 1.2 Hz). High signal-to-noise ratio face-selective responses were objectively (i.e., exactly at the face stimulation frequency) identified and quantified throughout the whole VOTC. Face-selective responses were widely distributed across the whole VOTC, but also spatially clustered in specific regions. Among these regions, the lateral section of the right middle fusiform gyrus showed the largest face-selective response by far, offering, to our knowledge, the first supporting evidence of two decades of neuroimaging observations with direct neural measures. In addition, three distinct regions with a high proportion of face-selective responses were disclosed in the right ventral anterior temporal lobe, a region that is undersampled in neuroimaging because of magnetic susceptibility artifacts. A high proportion of contacts responding only to faces (i.e., "face-exclusive" responses) were found in these regions, suggesting that they contain populations of neurons involved in dedicated face-processing functions. Overall, these observations provide a comprehensive mapping of visual category selectivity in the whole human VOTC with direct neural measures.

face perception | intracerebral recordings | fast periodic visual stimulation | face selectivity | fusiform gyrus

A brief glance at a face provides a wealth of information about a person's identity, emotional state, sex, age, attractiveness, and other important cues for social communication. Hence, being able to identify a face as a face and distinguish it from multiple variable nonface objects (i.e., face categorization) is a prerequisite for understanding all face-perception functions. The functional definition of brain regions supporting face categorization in humans has been investigated extensively as a primary research goal, and these findings may serve as a rich model for understanding perceptual categorization and brain organization in general.

Postmortem brain autopsies and structural imaging of individuals with face-recognition impairment after brain damage (i.e., prosopagnosia) (1, 2) point to a large territory of the human ventral occipito-temporal cortex (VOTC), from the occipital pole to the temporal pole, with a right hemispheric advantage, as the neural basis of face categorization (refs. 3–7; for recent reviews, see refs. 8 and 9). In the normal human brain, functional neuroimaging has been the primary method for investigating the neural basis of face categorization, first with positron emission tomography (PET) (10) and then with functional MRI (fMRI) (11, 12). Collectively, these studies have reported larger brain responses to face images than other visual objects in clusters, patches, or functional regions of a few cubic millimeters within the human VOTC (e.g., refs. 10–16). The clusters consistently reported across studies are localized in the lateral part of the middle/posterior fusiform gyrus [fusiform face area (FFA)] (12) and in the lateral part of the inferior occipital gyrus [occipital face area (OFA)] (17), as well as in the posterior superior temporal sulcus, a region that may be involved in more general and dynamic social communication functions (18). In right-handed individuals at least, these face-selective regions are typically larger in the right than the left hemisphere (14, 19). More recently, some fMRI studies have defined two face-selective regions in the lateral part of the middle/posterior fusiform gyrus (FFA1 and FFA2) (15) and one in the anterior temporal lobe (fATL) (14, 20–23).

Each of these regions is thought to have a definite function, or computational role, as a node in a vast network of face-selective areas (8, 13). However, fMRI provides only a hemodynamic (i.e., indirect) measure of neural activity, suffering from wide variations in signal-to-noise ratio (SNR) across brain regions, which has important consequences. For instance, the heterogeneous magnetic susceptibility of the local anatomy causes a strong signal dropout in the anterior VOTC (22, 24) so that fMRI studies may fail to report genuine face-selective responses in this region (25), and category selectivity in general is often limited to the posterior section of the VOTC (15). Moreover, smaller, scattered, face-selective responses in the VOTC may be entirely missed by

Significance

Understanding the neural basis of face perception, arguably the most important visual function for human social ecology, is of the utmost importance. With an original fast periodic visual stimulation approach, we provide a comprehensive quantification of selective brain responses to faces throughout the ventral visual stream with direct recordings in the gray matter. Selective responses to faces are distributed in the whole ventral occipito-temporal cortex, with a right hemispheric and regional specialization supporting two decades of indirect recordings of human brain activity in neuroimaging. We also disclose three distinct face-selective regions in the anterior temporal lobe, an undersampled region in neuroimaging, and reveal exclusive responses to faces at the neural population level in these regions.

Author contributions: J.J., C.J., and B.R. designed research; J.J., C.J., J.L.-S., H.B., and S.C.-C. performed research; C.J. contributed new reagents/analytic tools; J.J. and C.J. analyzed data; and J.J., C.J., J.L.-S., L.M., and B.R. wrote the paper.

The authors declare no conflict of interest.

This article is a PNAS Direct Submission. A.P. is a Guest Editor invited by the Editorial Board.

Data deposition: The intracranial electroencephalographic data have been deposited in the Dryad Digital Repository, datadryad.org (doi: 10.5061/dryad.5f9v7).

[1]J.J. and C.J. contributed equally to this work.

[2]To whom correspondence should be addressed. Email: bruno.rossion@uclouvain.be.

This article contains supporting information online at www.pnas.org/lookup/suppl/doi:10.1073/pnas.1522033113/-/DCSupplemental.

fMRI studies that identify only sufficiently large clusters of activation near blood vessels. More generally, these variations in SNR make it impossible for neuroimaging studies to identify, quantify, and thus compare face-selective responses across the whole human VOTC.

To date, the only alternative approach to clarify this issue is afforded by field potentials recorded in awake patients implanted with intracranial electrodes along the ventral and lateral occipitotemporal cortex (26, 27). These relatively rare (i.e., compared with neuroimaging) intracranial electroencephalographic (iEEG) recordings offer a unique opportunity to measure direct local neural activity with a very high SNR. iEEG studies comparing faces and nonface objects have recorded face-selective responses in widely distributed regions of the VOTC and made a number of important observations for understanding the neural basis of face categorization (26–34). However, even when large samples of participants are tested, face-selective responses are broadly distributed in the VOTC, without evidence of a clustered organization as found in fMRI (27, 30, 34). Thus, even though a good correlation between fMRI and iEEG face-selective responses has been shown in specific cortical regions of a few participants (35–39), the dominant role of the posterior fusiform gyrus (FG) and inferior occipital gyrus (IOG), and of the right hemisphere, in face categorization, has never been validated by direct measures of neural activity. More generally, although iEEG recordings do not suffer from regional variations in SNR, direct neural face-selective responses have not been localized, quantified, and compared across anatomical regions of the human VOTC.

Up to now, beyond the intrinsic difficulty of such studies and the limited availability of implanted patients, the major obstacle against a cartography of face selectivity at a large anatomical field of view in the VOTC has been the lack of objectivity in the definition of iEEG face-selective responses. For instance, increases of neural activity to faces compared with nonface objects can be found at various time scales, both in low-frequency responses time-locked and phase-locked to the stimulus [i.e., event-related potentials (ERPs), such as the N200/N170 component (27, 31, 36, 40)] and in non-phase-locked high-frequency electrophysiological activity [high-frequency broadband, i.e., gamma activity (29, 30, 33–35, 40)]. In the latter case, relevant frequency bands vary substantially across recording sites, individual brains, and time windows, making it virtually impossible to objectively define, quantify, and compare face-selective responses across different brain regions.

A potential powerful approach to overcome this problem is to stimulate the human brain at a fast fixed frequency rate for a prolonged time, a rather old stimulation method (41) best known for the type of electrophysiological responses that it generates, the "steady-state visual evoked potentials", on the scalp (42). The main advantages of this approach are its extremely high SNR, providing significant responses in a few minutes of stimulation or less, and its objectivity: The neural response of interest concentrates in the EEG exactly and exclusively at the known frequency rate of stimulation and its harmonics (42, 43). To our knowledge, the application of this approach in intracerebral recordings is rare (37, 44) and has not been used to address the issue of category selectivity.

Here, we use this fast periodic visual stimulation (FPVS) approach to report a comprehensive definition and quantification of face-selective responses across the VOTC in a large group of participants (n = 28) implanted with intracerebral electrodes. Using a paradigm recently validated in human adults (45) and infants (46), participants were shown sequences (70 s) of widely variable natural images of multiple object categories presented at a rapid periodic rate of six images per second (6 Hz). Images of faces were presented as every fifth image (Fig. 1 *A* and *B*). In this design, the common neural response to faces and nonface objects projects to the 6-Hz base rate. However, if faces elicit a differential neural response compared with all other categories, it will appear exactly at the experimentally defined frequency (i.e., 6 Hz/5 = 1.2 Hz). Thus, irrespective of the presence and magnitude of a 6-Hz response, a response at 1.2 Hz indicates category selectivity for faces, or face selectivity. This face-selective response can be objectively defined (i.e., at a known stimulation frequency) without subtraction across conditions (45) and quantified within anatomical regions throughout the whole VOTC, providing a cartography of category (face) selectivity in the human brain.

Results

A total of 192 electrode arrays, each containing 5–18 contiguous recording contacts, were implanted in the VOTC of 28 participants (44 individual hemispheres). These electrodes contained 1,678 individual recording contacts in the gray matter (left hemisphere, 988; right hemisphere, 690) (see Fig. 1*C* for typical electrode trajectories). In the frequency domain, responses occurring at 6 Hz and harmonics reflect the common response to faces and nonface stimuli (i.e., general visual response) whereas responses at 1.2 Hz and harmonics (2.4 Hz, 3.6 Hz, etc.) reflect face-selective responses (Fig. 1*A*) (45). A contact was considered as face-selective if a significant response was found at one or more of the first four face stimulation frequency harmonics.

Despite the brief recording time (two or four sequences of 70 s), high SNR face-selective responses were recorded in the VOTC exactly at 1.2 Hz and harmonics (see Fig. 2*A* for an example of

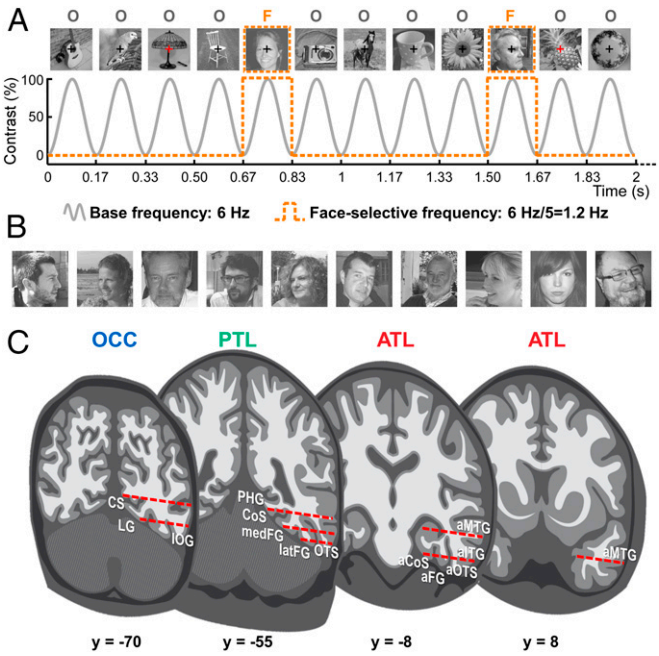

Fig. 1. FPVS and SEEG methods. (*A*) The FPVS paradigm. Images of objects were presented by sinusoidal contrast modulation at a rate of six stimuli per second (6 Hz). In the periodic condition shown here, a different face image was presented every five stimuli (i.e., appearing at the frequency of 6/5 = 1.2 Hz). (*B*) Representative examples of natural face images used in the study (actual images not shown for copyright reasons). Faces were embedded in their natural backgrounds and varied in size, viewpoint, and lighting conditions (50 face exemplars were used in total). (*C*) Schematic representation of the typical trajectories of depth electrodes (SEEG) implanted in the right VOTC. Intracerebral electrodes consist of 8–15 contiguous recording contacts spread along the electrode length, along the medio-lateral axis. Typical trajectories of electrodes are represented as arrays of red rectangles on schematic coronal slices (with Talairach *y* coordinates indicated below slices). Electrodes penetrate both gyral and sulcal cortical tissues. a, anterior; CS, calcarine sulcus; lat, lateral; LG, lingual gyrus; med, medial; PHG, parahippocampal gyrus.

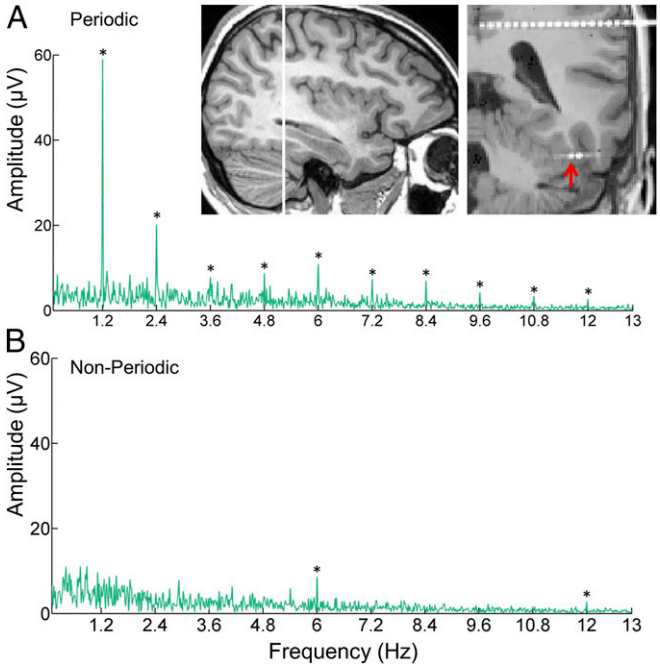

Fig. 2. Objective and high-SNR intracerebral responses in the VOTC. iEEG frequency-domain responses recorded at an individual recording contact (raw FFT amplitude) located in the right latFG (participant 14) are shown. The location of the recording contact (indicated by a red arrow) is shown using a postoperative CT coregistered to a preoperative MRI. (*A*) In the periodic condition, significant face-selective responses exactly at the face-selective frequency (1.2 Hz) and harmonics (up to 10.8 Hz) were observed. Note the high SNR of these responses (i.e., high amplitude at the specific frequency compared with the neighboring frequency bins), despite the brief recording time (two sequences of 70 s here). (*B*) In the nonperiodic condition, no face-selective responses were observed. In both conditions, general visual responses occurring exactly at the base frequency (6 Hz) and harmonics were recorded, with comparable amplitudes and SNR across conditions. *$z > 3.1$; $P < 0.001$.

recording in the right FG). In a nonperiodic condition (where the exact same stimuli were shown in random order, with no face periodicity), there were no contacts with significant responses at 1.2 Hz and harmonics (Fig. 2*B*), even though the 6-Hz general visual response was comparable to that observed in the periodic condition.

Spatial Distribution of Face-Selective Responses in the VOTC. Across the VOTC, we found a high proportion of face-selective contacts (33.1%; 555 of 1,678), with no difference between the left and right hemispheres (left: 313 of 988, 31.7%; right: 242 of 690, 35.1%; $P = 0.146$, Pearson's χ^2 test). These contacts were found in many regions of the occipital and temporal lobes and were widely distributed along the VOTC (Fig. 3*A*; see also Fig. S1*A* for the spatial relationship with contacts showing only a significant general visual response). The anatomical location of each face-selective contact was determined in the individual anatomy by using a topographic parcellation of the VOTC based on predefined well-established anatomical landmarks [Fig. S2; see also Fig. S1*B* for the spatial distribution of face-selective contacts in the Montreal Neurological Institute (MNI) space labeled according to their location in the individual anatomy]. Then, contacts were grouped by anatomical region of interest across all participants (Fig. 4). Table 1 shows the number of contacts in each of these regions (individual brains were not normalized, but see Table S1 for the coordinates of these regions in the MNI and Talairach spaces).

Fig. 4 displays the averaged iEEG frequency spectra in each region of the right hemisphere (see Fig. S3 for the left hemisphere). In the occipital lobe (OCC), face-selective responses were recorded in the IOG and in a large portion of the ventral and medial occipital cortex. Responses in the ventro-medial occipital cortex were distributed over multiple anatomical regions and were generally small relative to large general visual responses. Therefore, for sake of simplicity, these responses were grouped into the same region of interest [ventromedial occipital (VMO), comprising the occipital part of the CoS, the lingual gyrus, the calcarine sulcus, the cuneus, and the occipital pole].

In the posterior temporal lobe (PTL), face-selective responses were mainly recorded in the middle FG. The middle FG is divided longitudinally by the midfusiform sulcus in its medial and lateral sections (15). We recorded face-selective responses in the medial FG and adjacent CoS (medFG) and in the lateral FG and adjacent occipito-temporal sulcus (latFG). Face-selective responses

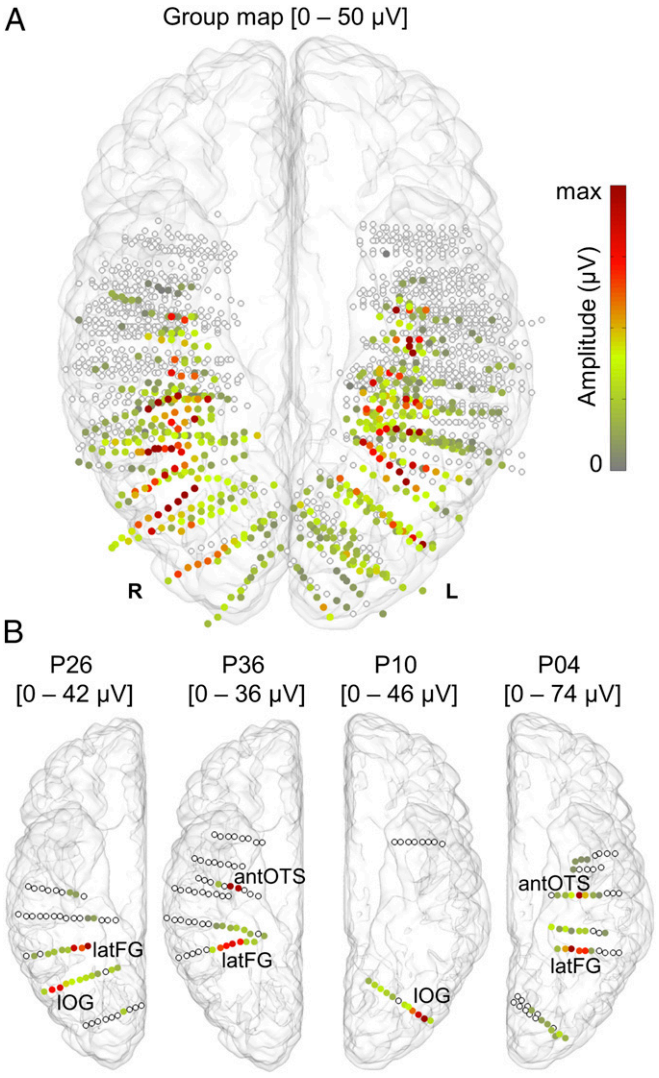

Fig. 3. Spatial distribution of face-selective contacts in the MNI space (ventral view). (*A*) Map of all 1,678 VOTC recording contacts across the 28 individual brains displayed in the MNI space using a transparent reconstructed cortical surface of the Colin27 brain. Each circle represents a single contact. Colored circles correspond to face-selective contacts color-coded according to their face-selective response amplitude. White-filled circles correspond to contacts that are not face-selective. For visualization purposes, individual contacts are displayed larger than their actual size (2 mm in length). (*B*) Examples of four individual participant hemispheres. Anatomical labels of the face-selective clusters in each participant are derived from the individual native anatomy.

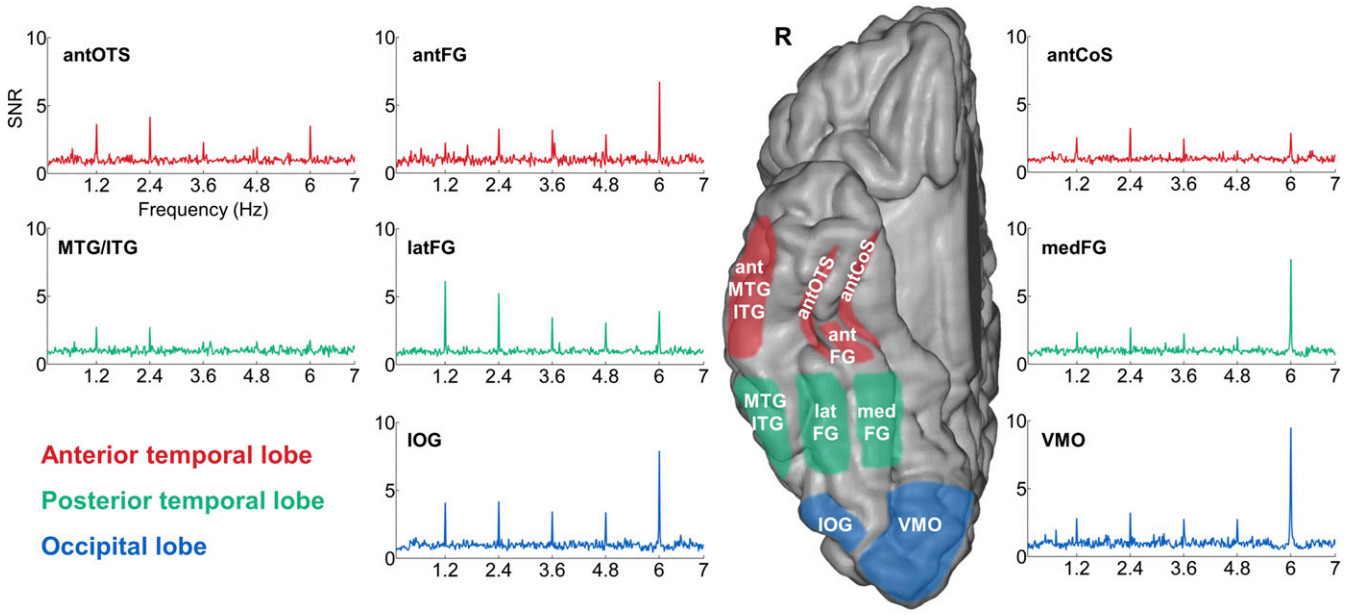

Fig. 4. Face-selective responses in distinct anatomical VOTC regions. iEEG SNR frequency spectra in each region of the right hemisphere averaged across all face-selective contacts located in the same region. SNR is computed by comparing amplitude at the frequency bin of interest to amplitude at neighboring bins (i.e., SNR = 1, no signal above noise level). The schematic locations of each region are shown on a reconstructed cortical surface of the Colin27 brain. For simplicity, regions are depicted over the cortical surface although responses were recorded within the cortex. Note the particularly large (i.e., high SNR) face-selective response recorded in the latFG and to a lesser extent in the IOG compared with other regions. Although face-selective contacts were found in the right antMTG/ITG (Fig. 8*A*), no clear responses were visible on the averaged spectrum, which is therefore not shown. Note that we did not record in the most posterior (in the OCC) and anterior parts of the FG.

were also recorded more laterally in the inferior temporal gyri (ITG) and middle temporal gyri (MTG).

In the anterior temporal lobe (ATL), face-selective responses were mainly recorded in the ventral ATL in three distinct regions: (*i*) along the anterior segment of the collateral sulcus (antCoS); (*ii*) along the anterior segment of the occipito-temporal sulcus [antOTS; located laterally to the CoS (47)]; and (*iii*) in the anterior FG [antFG; located between the antCoS and the antOTS, anteriorly to the posterior tip of the hippocampus (HIP) (25, 48)]. Fig. 5 displays typical recordings from the ventral ATL, as well as their precise anatomical locations in a single participant (P16). Face-selective responses were also recorded more laterally in the anterior part of the MTG and ITG (antMTG/ITG).

In summary, we recorded high-SNR face-selective responses in many regions of the VOTC, extending from the occipital pole to the ATL. These face-selective responses were particularly large in the latFG and IOG (Fig. 4). The general visual responses at 6 Hz were predominant in the OCC, medFG, and antFG.

Quantification of Face-Selective Response Amplitudes. To quantify and compare response amplitudes across regions, we summed the baseline-subtracted amplitudes over harmonics for each face-selective contact, separately for the face-selective responses (sum of the 12 first face-selective frequency harmonics, excluding the 5th and 10th harmonics that coincided with the base frequency) and for the general visual responses (sum over the first four base frequency harmonics). We averaged across contacts to obtain the mean response amplitude for each type of response and region.

Across all regions, the largest face-selective response, by far, was recorded in the right latFG (Fig. 6). This right latFG response was significantly larger than in all other regions taken independently ($P < 0.05$, two-tailed permutation test) (*SI Text*), except for the right antFG, which had the second largest response together with the right IOG (Fig. 6 and Table S2). Strikingly, the mean Talairach coordinates of the face-selective responses found in the right latFG ($x = 41$, $y = -45$, $z = -16$) (Table 2) and in the right IOG ($x = 43$, $y = -71$, $z = -7$) match the coordinates of face-selective clusters found with fMRI in these regions [right FFA and right OFA, respectively; e.g., ref. 14; right FFA average Talairach coordinates in a study with a large sample of participants: $x = 38$, $y = -43$, and $z = -17$ (14)]. The largest general visual responses were recorded in the OCC (VMO and IOG), in the medFG and in the antFG, whereas the smallest responses were recorded in the MTG/ITG and in the ATL (antCoS, antOTS, and antMTG/ITG) (Fig. 6). Note that the results of the quantification analysis were independent of the number of harmonics included in the analysis (Fig. S4*A*).

Although the proportion of face-selective contacts did not differ between right and left latFG (left: 30 of 36, 83.3%; right: 33 of 35, 94.3%; $P = 0.144$, Pearson's χ^2 test), there was a significantly

Table 1. Number of contacts showing face-selective responses in each anatomical region

Regions	Left hemisphere	Right hemisphere	Total
VMO	89 (7)	50 (5)	139 (11)
IOG	26 (6)	36 (6)	62 (11)
Subtotal OCC	115 (7)	86 (6)	201 (12)
medFG	40 (11)	30 (8)	70 (17)
latFG	30 (11)	33 (8)	63 (17)
MTG/ITG	30 (7)	25 (8)	55 (13)
Subtotal PTL	109 (13)	96 (11)	188 (21)
antCoS	33 (11)	23 (9)	56 (18)
antFG	10 (4)	11 (4)	21 (7)
antOTS	35 (12)	17 (5)	52 (15)
antMTG/ITG	20 (7)	17 (8)	37 (12)
Subtotal ATL	107 (16)	79 (15)	166 (23)
Total	313 (21)	242 (17)	555 (28)

The corresponding number of participants in which these face-selective contacts were found is indicated in parentheses.

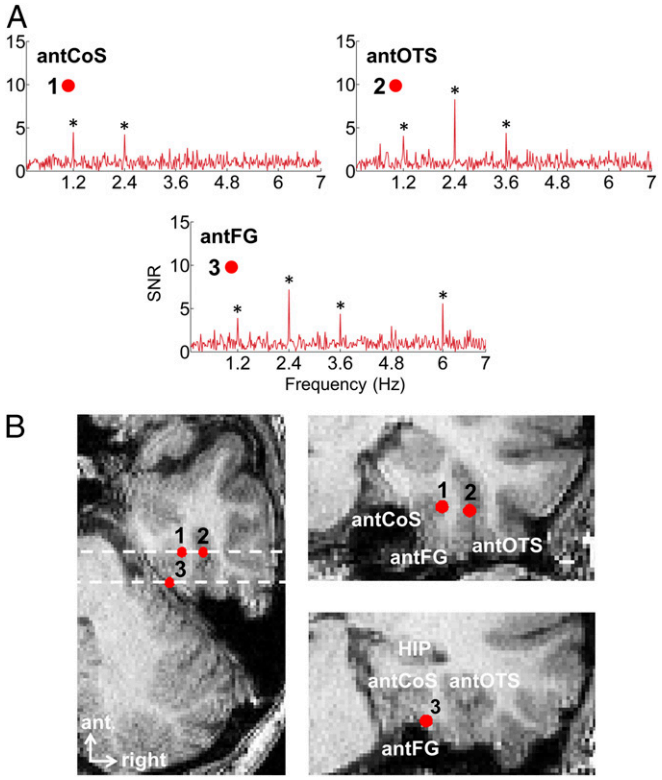

Fig. 5. Example of face-selective responses in three distinct anatomical regions of ventral ATL. (*A*) Face-selective responses recorded from the right antCoS, antOTS, and antFG in a single brain (participant 16). Note that in the antCoS and antOTS, no general visual responses were recorded at 6 Hz and harmonics (face-exclusive responses; see also Fig. 8*A*). *$z > 3.1$; $P < 0.001$. (*B*) Anatomical locations of corresponding recording contacts on MRI slices. Contacts are shown as red dots on axial (*Left*) and coronal (*Right*) slices. Electrode contacts 1, 2, and 3 are respectively located in the antCoS, antOTS, and antFG. The antFG is located between the antCoS and antOTS, at a level where the HIP is visible on a coronal slice.

larger face-selective response in the right latFG (mean difference: 26.03 μV) (Fig. 6; see Table 2 for results of the permutation tests). However, the general visual response did not differ between these two regions (Fig. 6 and Table 2). The IOG also showed a nonsignificant trend toward a larger face-selective response in the right hemisphere (Fig. 6 and Table 2).

In the ventral ATL, the face-selective response was larger in the antFG than in its adjacent sulci (antOTS and antCoS) in the right hemisphere only ($P < 0.05$). The general visual response was also larger in the antFG than in the antOTS and antCoS in both hemispheres ($P < 0.05$).

Because of the very high frequency resolution, the analysis used here is highly resistant to (intracerebral) artifacts (mainly epileptic spikes), which are more broadly distributed across the frequency spectrum than the specific frequencies of visual stimulation (37, 42). Nevertheless, to test for the robustness of the results, we performed the same quantification analysis after artifact rejection (*SI Text*). This complementary analysis yielded virtually identical results to those without artifact rejection (Fig. S5).

Clustered Spatial Organization of Face Selectivity in VOTC. Face-selective responses were widely distributed across the VOTC, with the largest responses found in specific anatomical regions of the right hemisphere. Because of the high spatial resolution of the SEEG approach (in the present study, the intercontact center-to-center spacing is 3.5 mm, whereas it is 5–10 mm in recent electrocorticography or ECoG studies) (e.g., refs. 35 and 49), we were also able to explore the spatial organization of face-selective responses at a finer scale within the different face-selective regions.

To do so, we first visualized face selectivity at single contacts within individual brains (see Fig. 3*B* for examples of four individual brains). We observed that face-selective contacts along an electrode (i.e., array of recording contacts mainly in the medio-lateral axis) tend to be spatially contiguous. This finding was reflected in the mean number of contiguous face-selective contacts (OCC, 4.3 ± 3.6 contacts; PTL, 4.9 ± 3.5; ATL, 2.6 ± 1.9; both hemispheres grouped) and in the mean distances between face-selective contacts (OCC, 5.1 ± 3.2 mm; PTL, 4.1 ± 0.9; ATL, 5.5 ± 4.2) which were significantly different from when randomly shuffling the contact location ($P < 0.01$ for all comparisons) (*SI Text*).

We also observed that, among face-selective contacts, the contacts with the largest face-selective amplitude tended to be spatially contiguous. This finding is exemplified in Fig. 3*B*, where the largest face-selective responses were grouped in specific regions (latFG, antOTS, and IOG). Highly face-selective contacts were defined for each electrode separately as contacts with a distinctively high amplitude (i.e., amplitude >3 SDs from the amplitude of the lowest contacts) (*SI Text*). The proportion of electrodes containing highly face-selective contacts was maximal in the antCoS, antFG, antOTS, medFG, latFG, and IOG, while being smaller in the VMO or equal to zero in the remaining regions (Fig. 7*A*; both hemispheres grouped). Among these electrodes, the mean distance between these contacts was significantly smaller than when randomly shuffling their positions on the electrodes (Fig. 7*B* and *SI Text*), showing that highly face-selective contacts tended to spatially cluster.

To further visualize and examine the spatial clustering of highly face-selective responses in each anatomical region, we quantified the spatial variation of face-selective response amplitude across the length of each electrode (*SI Text*). The profiles displayed in

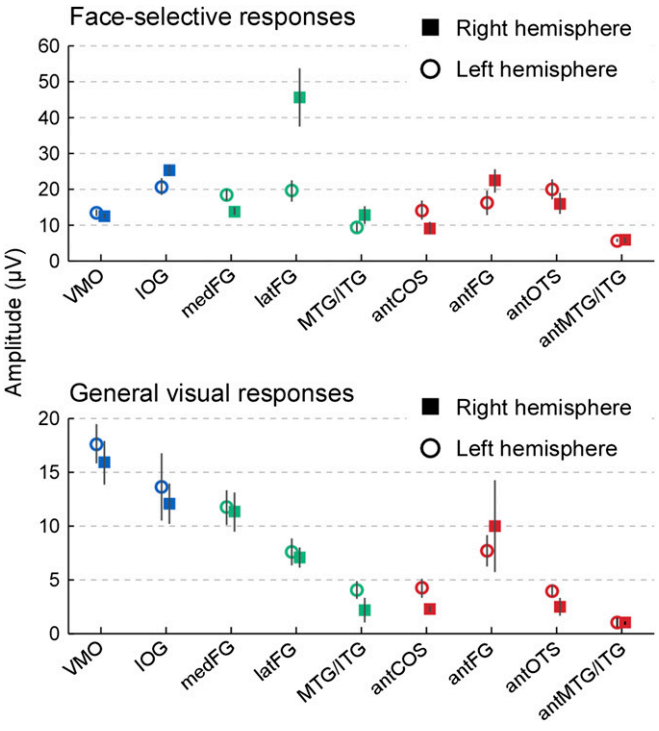

Fig. 6. Quantification of the response amplitudes in each region. Face-selective (*Upper*) and general visual (*Lower*) responses were quantified in each region as the average of the response amplitudes across contacts. The average across contacts for each region is shown separately for the left and right hemispheres. Error bars represent the SEM across contacts.

Table 2. Statistical comparisons between right and left hemisphere homologous regions using a permutation test

	Face-selective response		General visual response	
Regions	Mean difference R-L (μV)	*P* value	Mean difference R-L (μV)	*P* value
VMO	−0.93	0.526	−1.71	0.542
IOG	4.49	0.112	−1.56	0.657
medFG	−4.68*	0.020	−0.43	0.840
latFG	26.03*	0.001	−0.53	0.723
MTG/ITG	3.41	0.205	−1.83	0.187
antCoS	−4.93	0.165	−1.96	0.097
antFG	6.15	0.219	2.34	0.628
antOTS	−3.90	0.400	−1.49	0.165
antMTG/ITG	0.12	0.904	−0.05	0.914

See *SI Text* for details. L, left; R, right. *$P < 0.05$.

Fig. 7*C* represent the mean variation of face-selective response amplitude as a function of the distance from the maximum amplitude in each region (averaging both sides around the maximum and pooling across hemispheres to increase the number of data points). In most regions (except in MTG/ITG and antMTG/ITG), the second or third largest responses were contiguous to the maximum and significantly above the amplitude expected by chance if the contacts were randomly located (i.e., 95% confident interval) (Fig. 7*C*, gray area). This finding indicates that the largest face-selective responses tend to cluster in specific regions.

Face-Exclusive Responses. Strikingly, some individual recording contacts in the VOTC exhibited exclusive responses to faces—i.e., significant face-selective responses without any general visual response (for examples, see Fig. 8*A*). There were few face-exclusive responses in the occipital cortex (15, mainly in the IOG), 38 in the PTL (mainly in the MTG/ITG and in the latFG), and 58 in the ATL (mainly in the antOTS, antCoS, and antMTG/ITG). The proportion of face-exclusive contacts (with respect to all face-selective contacts) increased from posterior to anterior regions (Fig. 8*B*) and was maximal in the right ATL (30 of 68; 44.1%). In the ATL only, the proportion of face-exclusive contacts was significantly higher in the right than in the left hemisphere (44.1% vs. 28.6% respectively; $P = 0.039$, Pearson's χ^2 test).

To rule out the possibility that the higher proportion of face-exclusive responses in the ATL was merely due to this region's inability to generate responses at a fast rate (i.e., 6-Hz base rate), 11 of the participants performed a control experiment in which the exact same stimuli were presented at a slower base frequency rate (1.5 Hz) (*SI Text*). The reduction of general visual responses from posterior to anterior regions was similar whether we used 1.5 or 6 Hz as the base stimulation frequency (Fig. S4*B*). Moreover, the disappearance of the general visual responses on some contacts was not due to a global amplitude reduction, which would have affected first the general visual response because it is lower than face-selective response to begin with ("floor effect"). Indeed, we observed a similar reduction of general visual responses from posterior to anterior regions when general responses were extracted from groups of contacts with similar mean face-selective response amplitudes across regions (Fig. S4*C*).

Summary. In quantifying face selectivity across the whole human VOTC with intracerebral recordings and a high-sensitivity stimulation approach in a large group of individual brains, we made a number of key observations regarding the neural basis of face categorization. First, in line with human intracranial recording studies, we reported face-selective responses across all of the VOTC. Second, we validated two decades of functional neuroimaging findings with a direct measure of neural activity: Among all VOTC regions, the right latFG, corresponding to the right FFA, shows the largest face-selective response, followed by the right IOG (OFA). Third, we found different spatial organizations of face-selective responses across regions, with the key regions (i.e., IOG, latFG, and ATL regions) showing a clustered organization of highly face-selective responses. Fourth, we identified three regions exhibiting face-selective responses in the ventral ATL, specifically the antCoS, the antFG, and the antOTS. Finally, we report a number of face-exclusive responses at the population level, with these responses increasing along a posterior to anterior axis in the VOTC to reach almost 50% in the right ATL.

Discussion

Wide Distribution of Face-Selective Responses Across the VOTC. Besides the dominant latFG and IOG, face-selective responses were found in regions that are not, or are rarely, identified as face-selective in fMRI: the VMO, the medFG, the MTG/ITG, and in a large portion of the ventral ATL. These results are in line with

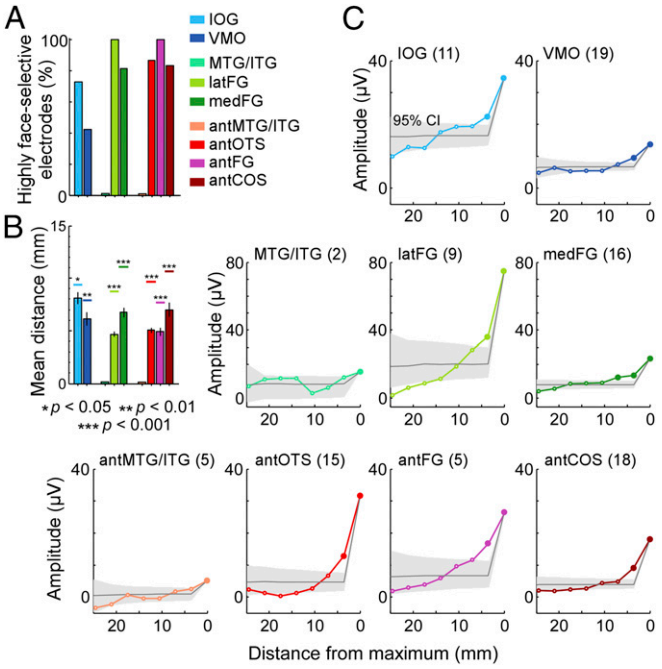

Fig. 7. Clustered organization of face selectivity within each region. (*A*) Proportion of electrodes showing highly face-selective contacts in each region. (*B*) Mean distance between highly face-selective contacts in electrodes highlighted in *A*. Error bars represent the SEM. These distances were significantly smaller than when randomly shuffling the locations of contacts on the electrodes (95% lower confidence interval indicated by horizontal lines). (*C*) Spatial variation of face-selective response amplitude in each region. All electrodes containing at least one face-selective contact were identified and pooled across hemispheres. The number of electrodes included in the analysis for each region is indicated in parentheses. Next, electrodes were spatially centered with respect to the contact recording the largest face-selective response. Each electrode was then folded around the maximum by averaging responses from equidistant contacts on both sides of the maximum. Face-selective responses measured at corresponding contacts across electrodes were then averaged by region. The resulting profiles represent the mean variation of face-selective response amplitude as a function of the distance from the maximum (maximum located at 0 mm). To statistically assess the clustering of highly face-selective responses in each region, these profiles were compared with a random distribution of profiles generated by repeatedly performing the exact same analysis after randomly shuffling the location of contacts in each electrode (i.e., both original and random profiles were spatially centered on the largest face-selective response). Shaded gray areas and thin gray lines, respectively, represent the 95% confidence interval and the mean of these random distributions. Face-selective responses above or equal to the 95% confidence interval are shown as larger filled markers.

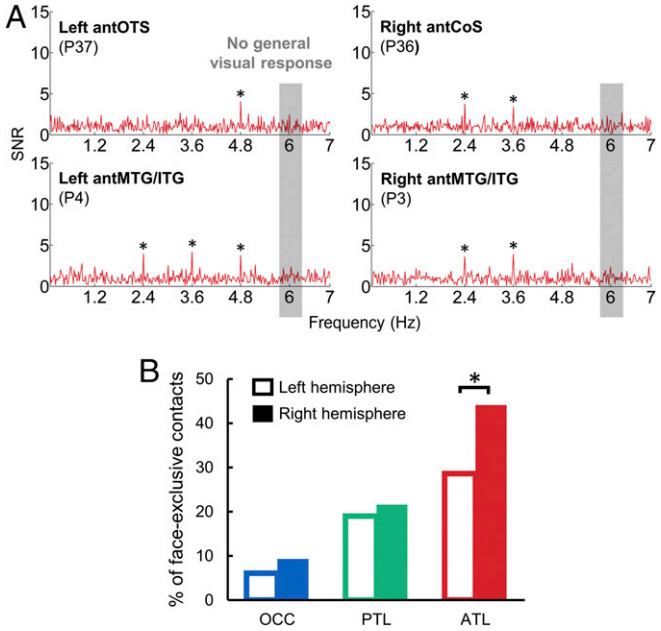

Fig. 8. Face-exclusive responses. (*A*) Examples of recordings in single participants in right and left ATL regions. *$z > 3.1$; $P < 0.001$. (*B*) Proportion of face-exclusive contacts. The proportion of face-exclusive contacts (with respect to all face-selective contacts) is displayed for the three main regions (OCC, PTL, and ATL). *$P < 0.05$ (Pearson's χ^2 test).

previous iEEG observations of widely distributed face-selective responses in the VOTC (27, 30, 33–35, 50). However, face-selective responses are even more extensively distributed here than previously observed, in particular compared with the seminal study of Allison et al. (27), using grids of electrodes on the cortical surface (ECoG). Moreover, our proportion of VOTC face-selective responses is larger than in previous studies. For example, whereas Allison et al. (27) reported 121 face-selective responses in 98 participants (N200: 82 responses, P350: 39 responses), we disclosed 555 face-selective responses in 28 participants.

Importantly, our wide distribution and high proportion of face-selective responses cannot reflect low-level visual differences between faces and nonface objects, not only because all images were equalized for mean pixel luminance and contrast. Most critically, the numerous natural images of face and object vary widely in lighting, contrast, size, viewpoint, etc. Thus, low-level cues do not vary systematically at the specific periodic rate of faces (1.2 Hz), eliminating the putative contribution of these cues to the measured face-selective response (45). Hence, face-selective responses in this stimulation mode disappear when images are phase-scrambled, preserving low-level visual cues (i.e., power spectrum; refs. 45 and 46). Moreover, with this approach, both generalization (across widely variable face exemplars) and discrimination (from widely variable nonface objects) are mandatory to elicit face-selective responses. Generalization is necessary because categorizing only a subset of the face stimuli as faces would break the 1.2-Hz periodicity. Discrimination of faces from each of the other object categories, not only from an average of their response as in a standard fMRI localizer (e.g., refs. 12, 16, and 51), is also necessary here. Indeed, if one of the nonface categories elicits the same response as faces, the 1.2-Hz periodicity will be disrupted. Finally, high selectivity to faces is ensured by using 14 nonface categories, a larger number than in previous studies, with a majority of studies comparing faces to a single nonface category (houses or cars typically; e.g., ref. 14; see also ref. 27 for 4–6 nonface categories in iEEG). Despite this control, and even though there is no other visual category than faces eliciting such a large specific response at the population level with such a right hemisphere advantage in the human brain, we cannot formally exclude the possibility that yet another visual category would also elicit category-specific 1.2-Hz responses in the VOTC if presented every fifth stimuli in our rapid visual stimulation sequence. Such a comparison of different category-selective response maps could be directly performed in future studies with the present FPVS approach.

Here we argue that two key aspects of the present study may account for the particularly large proportion and wide spatial distribution of face-selective responses identified. First, unlike ECoG (27), stereotactic electroencephalography (SEEG) records within cortical sulci, in which a substantial proportion of face-selective responses were found (i.e., CoS and OTS in the PTL and antCoS and antOTS in the ventral ATL). Second, we used a FPVS approach providing: (*i*) an objective criterion to identify even small neural responses above noise level in the frequency domain and (*ii*) an extremely high SNR compared with standard stimulation approaches (42, 43, 45). In summary, our results support the view that neural populations widely distributed across the human VOTC, rather than a few localized functional regions only as found in neuroimaging studies, generate robust selective responses to faces.

Regional Peaks of Face Selectivity. Although the right latFG shows the largest and most consistent face-selective response in human neuroimaging (e.g., refs. 8 and 12–14), previous iEEG studies did not identify this region as showing the largest face-selective response in the VOTC, because face-selective responses were not compared across regions (30, 34), the issue of FG lateralization was not addressed (35), or face-selective responses in the FG were not lateralized [ERPs (27); broadband gamma activity (40)]. Here, of all anatomically defined VOTC regions, the largest face-selective iEEG response was found in the lateral section of the right middle FG (latFG; Talairach coordinates: $x = 41$, $y = -45$, $z = -16$), which corresponds to the right FFA (10, 12). This observation therefore validates with a direct measure of neural activity the predominant face-selective activation in the right latFG found in human neuroimaging (i.e., the FFA) (12).

The larger face-selective response in the right than in the left latFG may be at least partly due to the spatial organization of face-selective neuronal populations. To record large face-selective responses on some contacts in the right latFG as here, a large number of face-selective neurons should be densely grouped nearby the recording contacts. Although we were not able to compare right and left latFG with our clustering analysis because of a low statistical power (6 and 3 electrodes peaking in right and left latFG, respectively), this hypothesis is supported by the dense clustered organization of highly face-selective responses found in the latFG when both hemispheres were grouped. In addition, although face-selective responses were also recorded in the medFG here, they were substantially smaller in amplitude than in the latFG. This observation supports the recently discovered cytoarchitectonic and fMRI-based functional mediolateral division of the FG (52).

The right hemispheric dominance of our electrophysiological measures is in line with the well-established dominance of this hemisphere in face perception as evidenced by divided visual field presentation (53), neuroimaging (e.g., refs. 10, 12, and 14) and scalp EEG (54), including studies performed with the same paradigm as used here (45, 46). Most importantly, our results agree with the localization of brain damage in patients with acquired prosopagnosia, whose lesions are either bilateral or localized unilaterally in the right hemisphere (refs. 2–7, except in a few left-handed patients: for review, see ref. 9), as well as with the right dominance of the lateral section of the middle FG in producing conscious distortions of a perceived face (38, 40).

Importantly, prosopagnosia can also be due to lesions of the right IOG (refs. 4 and 51; see also ref. 55 for face-processing

impairment due to transcranial magnetic stimulation over this region), as well as of the right ATL (56). In line with evidence from these lesion studies, here, the second largest face-selective responses were found in the right IOG and antFG, two regions in which highly face-selective responses were also clustered. The right IOG corresponds to the cortical territory where the OFA is typically located (16, 17, 51), so that our observations again validate the findings of neuroimaging studies of face perception. The right antFG is part of the ventral ATL, whose role in face perception is currently the focus of intense research (ref. 25; for review, see ref. 57) and which will be discussed next.

A Set of Face-Selective Regions in the ATL. Although the fMRI signal in the ventral ATL is absent or very weak, previous iEEG studies have found widely distributed face-selective responses in this region, yet without providing precise anatomical information (i.e., ref. 32). Here, we took advantage of the high spatial resolution of depth electrodes and their specific recordings of both gyri and sulci to clarify the locations of face-selective responses in the ventral ATL. We found a wide distribution of face-selective responses in the ventral ATL (antCoS, antFG, and antOTS) in specific and reproducible anatomical locations across individual participants. In these regions, we also found clusters of highly face-selective responses, even if their mean amplitude was not among the largest (except in the right antFG). This result is probably because our anatomical regions of interest were larger in size than the corresponding clusters.

Face selectivity in the antCoS is in line with the finding of face-selective responses in the anterior segment of the CoS bilaterally in a few relatively recent fMRI studies (14, 20–23, 58). Moreover, we found face-selective responses in the antOTS, which is a major VOTC sulcus, located laterally to the antCoS (47). Although the antOTS was never explicitly mentioned as a face-selective area in fMRI, visual analysis of individual data from these studies suggests that some anterior face-selective activations fall into the antOTS, and not into the antCoS as described (20, 22, 23). Our finding is also in agreement with ECoG studies reporting face-selective responses close to the antCoS and antOTS (27, 50). Given that antCoS and antOTS correspond to different cytoarchitectonic structures [perirhinal cortex and temporal isocortex, respectively (59)], these two regions may be functionally distinct and may support different face-selective neural processes.

The antFG is located anteriorly to the posterior FG and the typical location of the FFA (25, 48, 60). Unfortunately, because of magnetic susceptibility artifacts, fMRI signal recorded from this antFG region is absent or very weak (20–25). As a result, only a handful of fMRI studies reported face-selective activations in the antFG, and little is known about the role of this region in face processing (refs. 21, 23, and 58; but see ref. 61 for categorical differences between unfamiliar and familiar faces in the right antFG using PET). A recent iEEG study using depth electrodes recorded electrophysiological face-selective responses directly from the right antFG in a single participant (25). Electrically stimulating these intracerebral sites evoked transient prosopagnosia, pointing to a causal role of the right antFG in face recognition. Identifying clear iEEG face-selective responses specifically in this region in several individual brains here further supports its prominent role in human face recognition.

Accumulating data with the present approach over very large samples of individual brains, as well as refined anatomical definitions of the regions of interest (for example, based on cyto- or receptor-architectonics) (e.g., ref. 52) should progressively clarify the relative functional importance of these ATL regions in face categorization.

Face-Exclusive Responses Predominant in the Right ATL. Previous human iEEG studies recorded large responses to faces with weak responses to nonface stimuli over the VOTC (27, 50). Here, thanks to a clear definition of signal and noise provided by the fast periodic stimulation and the frequency domain analysis (43), we were able to objectively assess the absence of response (i.e., no signal above noise) to nonface objects at face-selective contacts. We found numerous face-selective responses in the absence of a general visual response. Such EEG spectra have not been found on the human scalp (45). Because intracerebral contacts pool the activity of hundreds of thousands of neurons, this finding reveals the presence of exclusive responses to faces at a macroscopic level of cortical organization (i.e., cell population level). Exclusive responses to the category of faces have been found in single neurons in the monkey superior temporal sulcus (62, 63), and there is evidence that these neurons are grouped in cortical columns or larger clusters (64) so that face-selective areas identified in fMRI in monkeys contain an extremely large proportion of neurons responding exclusively to faces (64). Here, to our knowledge, we report the first evidence of face-exclusive responses at a cell-population level in humans.

The right ATL recorded the highest proportion of face-exclusive responses, suggesting that it is involved in the highest stages of face processing. Compared with face processes that require information about the context (e.g., face detection among visual scenes or other objects), processing faces independently from the context (i.e., nonface categories) may be particularly useful for processes that are known to be specific to faces (e.g., encoding and retrieval of information specific to an individual face, holistic processing of individual exemplars, sex, age, expression, social judgments, etc.). This suggestion is consistent with fMRI and brain lesions studies showing that right ATL may play a role in face individualization and semantic knowledge about people (10, 56, 65, 66).

Conclusions

Thanks to intracerebral recordings performed in a large human population and a fast periodic presentation of objects and faces, objective face-selective responses were defined and quantified by anatomical regions along the whole VOTC. Our findings reconcile two main views of the large-scale functional organization of face selectivity in the VOTC: on the one hand, the partial and clustered organization identified by fMRI studies and, on the other hand, the widely distributed, scattered face-selective responses found by iEEG studies. Although face-selective populations of neurons are present across the whole VOTC, they are more densely distributed in specific regions, such as the right latFG, which are typically identified in fMRI and may be the most critical regions for this function. Even though the frequency-tagging approach used here essentially concentrated on quantitative differences between regions, it also revealed a qualitative difference at a finer-scale level, with an increasing proportion of electrode contacts showing exclusive response to faces as one progresses from posterior to anterior VOTC regions, particularly in the right hemisphere. Taking advantage of this objective and sensitive approach, future studies with higher recording samples in each region may be able to extract significant information from the patterns of face-selective harmonic responses in amplitude and phase (i.e., the shape of the output function) in various VOTC regions, and make further progress in our understanding of the spatiotemporal dynamics of face categorization in the human brain.

Materials and Methods

Participants. The study included 28 right-handed participants (15 females, mean age: 30.5 ±4.4 y) undergoing clinical intracerebral evaluation with depth electrodes [SEEG (67)] for refractory partial epilepsy. Participants were studied in the Epilepsy Unit of the University Hospital of Nancy between December 2012 and March 2015. Participants were included in the study if they had at least one intracerebral electrode implanted in the temporal or occipital lobe and if they were right-handed (as assessed by the Edinburgh Handedness Inventory). They all gave written consent to participate to the

study, which was part of a protocol approved by the human investigation committee of the University Hospital of Nancy. All but two participants performed the Benton Face Recognition Test (68) before the SEEG exploration, with an average score of 41.8 ± 4.4 (20 participants above a score of 39 of 54, indicating normal performances in matching individual faces, and 6 participants below 39 of 54, indicating mild impairment).

Intracerebral Electrode Implantation and Recording. Intracerebral electrodes were stereotactically implanted within the participants' brains to delineate their seizure onset zone. Each intracerebral electrode consisted of a cylinder of 0.8 mm diameter and contained 8–15 independent recording contacts of 2 mm in length separated by 1.5 mm from edge to edge and by 3.5 mm center-to-center (for details about the electrode implantation procedure, see ref. 25). Typical trajectories of depth electrodes implanted in the temporal and occipital lobes are shown in Fig. 1*C*. Intracerebral EEG was recorded at a 512-Hz sampling rate with a 256-channel amplifier with either a midline prefrontal scalp electrode (FPz, in 21 participants) or an intracerebral contact in the white matter serving as reference electrode (in 7 participants).

FPVS Paradigm.

Stimuli. A total of 200 grayscale natural images of various nonface objects (from 14 nonface categories: cats, dogs, horses, birds, flowers, fruits, vegetables, houseplants, phones, chairs, cameras, dishes, guitars, and lamps) and 50 grayscale natural images of faces were used, and were the same as in a recent study (45) [see Fig. 1*B* for examples of various face exemplars (stimuli available at dx.doi.org/10.5061/dryad.5f9v7) and Fig. S6 for mean images for each category]. Each image contained an unsegmented object or face near the center that differed in terms of size, viewpoint, lighting conditions, and background. Images were equalized for mean pixel luminance and contrast.

Procedure. Participants viewed continuous sequences with highly variable natural images of objects presented at a rate of 6 Hz through sinusoidal contrast modulation (Fig. 1*A*). A sequence lasted 70 s, including 66 s of stimulation at full contrast flanked by 2 s of fade-in and fade-out, where contrast gradually increased or decreased, respectively. The long sequence duration produces a high-frequency resolution (sequences of 63 s long were taken into account in the analysis, yielding a frequency resolution of 1/63 = 0.016 Hz) that allows isolating the response of interest into a narrow frequency bin, which greatly enhanced its SNR (42, 43). The experiment consisted of two types of sequences: (*i*) periodic and (*ii*) nonperiodic. In the main condition (i.e., periodic), highly variable natural images of faces were presented periodically as every fifth image (i.e., at 1.2 Hz = 6/5 Hz), with all images being randomly selected from their respective categories (Fig. 1*A*; see also Movie S1 for an example of visual stimulation in the periodic condition). In the control condition (i.e., nonperiodic), the exact same stimuli were shown in random order so that there was no face periodic input at 1.2 Hz. Participants were unaware of the periodicity of the faces in the periodic condition. Each participant was presented with at least two sequences of the periodic condition and one sequence of the nonperiodic condition, in pseudorandom order (~5 min of experiment, including short breaks). The experiment was repeated a second time for 12 of 28 participants. No participant had seizures in the 2 h preceding FPVS recordings. During the sequences, participants were instructed to fixate on a small black cross which was presented continuously at the center of the stimuli and to detect brief (500 ms) color changes (black to red) of this fixation cross.

Intracerebral EEG Analysis.

Frequency domain processing. Segments of iEEG corresponding to stimulation sequences were extracted (74-s segments, −2 to +72 s). In our main analyses, no artifact rejection was performed because intracerebral artifacts (mainly epileptic spikes, but also electro-oculographic and electro-myographic activity because we used a prefrontal scalp electrode as reference electrode for most of the participants) are more broadly distributed across the frequency spectrum than the frequencies of interest (i.e., 1.2 and 6 Hz and their respective harmonics). The 74-s data segments were cropped to contain an integer number of 1.2-Hz cycles beginning 2 s after the onset of the sequence (right at the end of the fade-in period) until ~65 s, before stimulus fade-out (75 face cycles ~ 63 s). Sequences were averaged in the time domain, separately for each condition and each participant. Subsequently, a fast Fourier transform (FFT) was applied to these averaged segments, and amplitude spectra were extracted for all contacts.

Face-selective responses. The FPVS approach used here allows for identifying and separating two distinct types of responses (45): (*i*) a general visual response occurring at the base stimulation frequency (6 Hz) and its harmonics, as well as (*ii*) a face-selective response at 1.2 Hz and its harmonics. Face-selective responses significantly above noise level at the face stimulation frequency (1.2 Hz) and its harmonics (2.4, 3.6 Hz, etc.) were determined by transforming the frequency spectra to *z* scores (45, 69). The *z* scores were computed as the difference between amplitude at each frequency bin and the mean amplitude of the corresponding 48 surrounding bins (25 bins on each side, i.e., 50 bins, but excluding the 2 bins directly adjacent to the bin of interest, i.e., 48 bins) divided by the SD of amplitudes in the corresponding 48 surrounding bins. A contact was considered as face-selective if a *z* score was >3.1 (i.e., $P < 0.001$, one-tailed: signal > noise) for at least one of the first four face-selective frequency harmonics in the periodic condition (1.2, 2.4, 3.6, or 4.8 Hz; we considered it unlikely that face-selective responses would manifest only at harmonics above the 6-Hz base frequency).

Quantification of responses amplitude. Baseline-corrected amplitudes were computed as the difference between the amplitude at each frequency bin and the average of 48 corresponding surrounding bins (25 bins on each side, i.e., 50 bins, but excluding the 2 bins directly adjacent to the bin of interest, i.e., 48 bins) (e.g., ref. 70). The face-selective and general visual responses were then quantified at each face-selective contact as the sum of the baseline-subtracted amplitude across harmonics (70, 71). The range over which face and base frequency harmonics were summed was constrained by the highest significant harmonic across participants (*z* score > 3.1; $P < 0.001$). Across all participants, no significant face-selective response was found above the 14th harmonic (i.e., 16.8 Hz), and no significant base frequency responses was found above the 4th harmonic (i.e., 24 Hz). Face-selective responses were therefore quantified as the sum of the baseline-subtracted amplitudes at the face-selective frequency harmonics from the 1st until the 14th (1.2 until 16.8 Hz), excluding the 5th and 10th harmonics (6 and 12 Hz) that coincided with the base frequency. General visual responses were similarly quantified by summing the amplitudes from the 1st until the 4th base frequency harmonics (6 until 24 Hz). Thus, for each face-selective contact, we obtained two amplitude values that respectively represented the overall face-selective response and the overall general visual response. SNR spectra were also calculated as the ratio between the amplitude at each frequency bin and the average of the corresponding 48 surrounding bins for display purposes and comparison across studies.

Contact Localization in the Individual Anatomy. Rather than normalizing individual brains by linear transformation, which blurs the individuality of functional organization, we subdivided individual brains in anatomical regions of interest using individual anatomical landmarks (i.e., gyri and sulci) (Fig. S2). Individual face-selective contacts were then localized according to this anatomical subdivision and grouped by anatomical location across all participants. We used a topographic parcellation of the VOTC close to that proposed by Kim et al. (48). Major VOTC sulci served as medio-lateral landmarks (CoS and OTS), and coronal reference planes containing given landmarks served as postero-anterior landmarks (Fig. S2). A coronal plane including the anterior tip of the parieto-occipital sulcus served as the border of the occipital and temporal lobes. A coronal plane including the posterior tip of the HIP served as the border of PTL and ATL. In a separate analysis, anatomical MRIs were also spatially normalized to determine Talairach and MNI coordinates of intracerebral contacts.

ACKNOWLEDGMENTS. We thank the participants for their involvement in the study; Ernest Galbrun for helping coregistering brain images; and Talia Retter and two anonymous reviewers for their comments on a previous version of the manuscript. J.J., J.L.-S., and B.R. are supported by the Belgian National Fund for Scientific Research (FNRS) and C.J. is supported by the Belgian Federal Government (BELSPO, return grant 2012). This work was supported by European Research Council Grant facessvep 284025.

1. Bodamer J (1947) Die Prosop-agnosie; die Agnosie des Physiognomieerkennens. *Arch Psychiatr Nervenkr Z Gesamte Neurol Psychiatr* 118(1-2):6–53.
2. Quaglino A, Borelli GB, Della Sala S, Young AW (2003) Quaglino's 1867 case of prosopagnosia. *Cortex* 39(3):533–540.
3. Barton JJ (2008) Structure and function in acquired prosopagnosia: Lessons from a series of 10 patients with brain damage. *J Neuropsychol* 2(Pt 1):197–225.
4. Bouvier SE, Engel SA (2006) Behavioral deficits and cortical damage loci in cerebral achromatopsia. *Cereb Cortex* 16(2):183–191.
5. De Renzi E, Perani D, Carlesimo GA, Silveri MC, Fazio F (1994) Prosopagnosia can be associated with damage confined to the right hemisphere—an MRI and PET study and a review of the literature. *Neuropsychologia* 32(8):893–902.
6. Hécaen H, Angelergues R (1962) Agnosia for faces (prosopagnosia). *Arch Neurol* 7:92–100.
7. Meadows JC (1974) The anatomical basis of prosopagnosia. *J Neurol Neurosurg Psychiatry* 37(5):489–501.
8. Duchaine B, Yovel G (2015) A revised neural framework for face processing. *Annu Rev Vis Sci* 1:393–416.

9. Rossion B (2014) Understanding face perception by means of prosopagnosia and neuroimaging. *Front Biosci (Elite Ed)* 6:258–307.
10. Sergent J, Ohta S, MacDonald B (1992) Functional neuroanatomy of face and object processing. A positron emission tomography study. *Brain* 115(Pt 1):15–36.
11. Puce A, Allison T, Gore JC, McCarthy G (1995) Face-sensitive regions in human extrastriate cortex studied by functional MRI. *J Neurophysiol* 74(3):1192–1199.
12. Kanwisher N, McDermott J, Chun MM (1997) The fusiform face area: A module in human extrastriate cortex specialized for face perception. *J Neurosci* 17(11):4302–4311.
13. Haxby JV, Hoffman EA, Gobbini MI (2000) The distributed human neural system for face perception. *Trends Cogn Sci* 4(6):223–233.
14. Rossion B, Hanseeuw B, Dricot L (2012) Defining face perception areas in the human brain: A large-scale factorial fMRI face localizer analysis. *Brain Cogn* 79(2):138–157.
15. Weiner KS, Grill-Spector K (2010) Sparsely-distributed organization of face and limb activations in human ventral temporal cortex. *Neuroimage* 52(4):1559–1573.
16. Zhen Z, et al. (2015) Quantifying interindividual variability and asymmetry of face-selective regions: A probabilistic functional atlas. *Neuroimage* 113:13–25.
17. Gauthier I, et al. (2000) The fusiform "face area" is part of a network that processes faces at the individual level. *J Cogn Neurosci* 12(3):495–504.
18. Puce A, Allison T, Bentin S, Gore JC, McCarthy G (1998) Temporal cortex activation in humans viewing eye and mouth movements. *J Neurosci* 18(6):2188–2199.
19. Bukowski H, Dricot L, Hanseeuw B, Rossion B (2013) Cerebral lateralization of face-sensitive areas in left-handers: Only the FFA does not get it right. *Cortex* 49(9): 2583–2589.
20. Tsao DY, Moeller S, Freiwald WA (2008) Comparing face patch systems in macaques and humans. *Proc Natl Acad Sci USA* 105(49):19514–19519.
21. Rajimehr R, Young JC, Tootell RB (2009) An anterior temporal face patch in human cortex, predicted by macaque maps. *Proc Natl Acad Sci USA* 106(6):1995–2000.
22. Axelrod V, Yovel G (2013) The challenge of localizing the anterior temporal face area: A possible solution. *Neuroimage* 81:371–380.
23. Nasr S, Tootell RB (2012) Role of fusiform and anterior temporal cortical areas in facial recognition. *Neuroimage* 63(3):1743–1753.
24. Ojemann JG, et al. (1997) Anatomic localization and quantitative analysis of gradient refocused echo-planar fMRI susceptibility artifacts. *Neuroimage* 6(3):156–167.
25. Jonas J, et al. (2015) Beyond the core face-processing network: Intracerebral stimulation of a face-selective area in the right anterior fusiform gyrus elicits transient prosopagnosia. *Cortex* 72:140–155.
26. Halgren E, et al. (1994) Spatio-temporal stages in face and word processing. I. Depth-recorded potentials in the human occipital, temporal and parietal lobes [corrected]. *J Physiol Paris* 88(1):1–50; erratum in *J Physiol Paris* 1994; 88(2): following 151.
27. Allison T, Puce A, Spencer DD, McCarthy G (1999) Electrophysiological studies of human face perception. I: Potentials generated in occipitotemporal cortex by face and non-face stimuli. *Cereb Cortex* 9(5):415–430.
28. Barbeau EJ, et al. (2008) Spatio temporal dynamics of face recognition. *Cereb Cortex* 18(5):997–1009.
29. Davidesco I, et al. (2014) Exemplar selectivity reflects perceptual similarities in the human fusiform cortex. *Cereb Cortex* 24(7):1879–1893.
30. Engell AD, McCarthy G (2011) The relationship of γ oscillations and face-specific ERPs recorded subdurally from occipitotemporal cortex. *Cereb Cortex* 21(5):1213–1221.
31. Liu H, Agam Y, Madsen JR, Kreiman G (2009) Timing, timing, timing: Fast decoding of object information from intracranial field potentials in human visual cortex. *Neuron* 62(2):281–290.
32. Puce A, Allison T, McCarthy G (1999) Electrophysiological studies of human face perception. III: Effects of top-down processing on face-specific potentials. *Cereb Cortex* 9(5): 445–458.
33. Sato W, et al. (2014) Rapid, high-frequency, and theta-coupled gamma oscillations in the inferior occipital gyrus during face processing. *Cortex* 60:52–68.
34. Vidal JR, et al. (2010) Category-specific visual responses: An intracranial study comparing gamma, beta, alpha, and ERP response selectivity. *Front Hum Neurosci* 4:195.
35. Jacques C, et al. (2016) Corresponding ECoG and fMRI category-selective signals in human ventral temporal cortex. *Neuropsychologia* 83:14–28.
36. Jonas J, et al. (2012) Focal electrical intracerebral stimulation of a face-sensitive area causes transient prosopagnosia. *Neuroscience* 222:281–288.
37. Jonas J, et al. (2014) Intracerebral electrical stimulation of a face-selective area in the right inferior occipital cortex impairs individual face discrimination. *Neuroimage* 99: 487–497.
38. Parvizi J, et al. (2012) Electrical stimulation of human fusiform face-selective regions distorts face perception. *J Neurosci* 32(43):14915–14920.
39. Puce A, Allison T, Spencer SS, Spencer DD, McCarthy G (1997) Comparison of cortical activation evoked by faces measured by intracranial field potentials and functional MRI: Two case studies. *Hum Brain Mapp* 5(4):298–305.
40. Rangarajan V, et al. (2014) Electrical stimulation of the left and right human fusiform gyrus causes different effects in conscious face perception. *J Neurosci* 34(38):12828–12836.
41. Adrian ED, Matthews BH (1934) The Berger rhythm: Potential changes from the occipital lobes in man. *Brain* 4(57):355–385.
42. Regan D (1989) *Human Brain Electrophysiology: Evoked Potentials and Evoked Magnetic Fields in Science and Medicine* (Elsevier, New York).
43. Norcia AM, Appelbaum LG, Ales JM, Cottereau BR, Rossion B (2015) The steady-state visual evoked potential in vision research: A review. *J Vis* 15(6):4.
44. Winawer J, et al. (2013) Asynchronous broadband signals are the principal source of the BOLD response in human visual cortex. *Curr Biol* 23(13):1145–1153.
45. Rossion B, Torfs K, Jacques C, Liu-Shuang J (2015) Fast periodic presentation of natural images reveals a robust face-selective electrophysiological response in the human brain. *J Vis* 15(1):18.
46. de Heering A, Rossion B (2015) Rapid categorization of natural face images in the infant right hemisphere. *eLife* 4:e06564.
47. Huntgeburth SC, Petrides M (2012) Morphological patterns of the collateral sulcus in the human brain. *Eur J Neurosci* 35(8):1295–1311.
48. Kim JJ, et al. (2000) An MRI-based parcellation method for the temporal lobe. *Neuroimage* 11(4):271–288.
49. Matsuo T, et al. (2015) Alternating zones selective to faces and written words in the human ventral occipitotemporal cortex. *Cereb Cortex* 25(5):1265–1277.
50. Tanji K, Iwasaki M, Nakasato N, Suzuki K (2012) Face specific broadband electrocorticographic spectral power change in the rhinal cortex. *Neurosci Lett* 515(1):66–70.
51. Rossion B, et al. (2003) A network of occipito-temporal face-sensitive areas besides the right middle fusiform gyrus is necessary for normal face processing. *Brain* 126(Pt 11):2381–2395.
52. Weiner KS, Zilles K (2016) The anatomical and functional specialization of the fusiform gyrus. *Neuropsychologia* 83:48–62.
53. Hillger LA, Koenig O (1991) Separable mechanisms in face processing: Evidence from hemispheric specialization. *J Cogn Neurosci* 3(1):42–58.
54. Rossion B, Joyce CA, Cottrell GW, Tarr MJ (2003) Early lateralization and orientation tuning for face, word, and object processing in the visual cortex. *Neuroimage* 20(3): 1609–1624.
55. Pitcher D, Walsh V, Yovel G, Duchaine B (2007) TMS evidence for the involvement of the right occipital face area in early face processing. *Curr Biol* 17(18):1568–1573.
56. Busigny T, et al. (2014) Face-specific impairment in holistic perception following focal lesion of the right anterior temporal lobe. *Neuropsychologia* 56:312–333.
57. Collins JA, Olson IR (2014) Beyond the FFA: The role of the ventral anterior temporal lobes in face processing. *Neuropsychologia* 61:65–79.
58. Pyles JA, Verstynen TD, Schneider W, Tarr MJ (2013) Explicating the face perception network with white matter connectivity. *PLoS One* 8(4):e61611.
59. Braak H, Braak E (1985) On areas of transition between entorhinal allocortex and temporal isocortex in the human brain. Normal morphology and lamina-specific pathology in Alzheimer's disease. *Acta Neuropathol* 68(4):325–332.
60. Onitsuka T, et al. (2003) Fusiform gyrus volume reduction and facial recognition in chronic schizophrenia. *Arch Gen Psychiatry* 60(4):349–355.
61. Rossion B, Schiltz C, Robaye L, Pirenne D, Crommelinck M (2001) How does the brain discriminate familiar and unfamiliar faces?: A PET study of face categorical perception. *J Cogn Neurosci* 13(7):1019–1034.
62. Gross CG, Rocha-Miranda CE, Bender DB (1972) Visual properties of neurons in inferotemporal cortex of the macaque. *J Neurophysiol* 35(1):96–111.
63. Desimone R (1991) Face-selective cells in the temporal cortex of monkeys. *J Cogn Neurosci* 3(1):1–8.
64. Tsao DY, Freiwald WA, Tootell RB, Livingstone MS (2006) A cortical region consisting entirely of face-selective cells. *Science* 311(5761):670–674.
65. Nestor A, Plaut DC, Behrmann M (2011) Unraveling the distributed neural code of facial identity through spatiotemporal pattern analysis. *Proc Natl Acad Sci USA* 108(24):9998–10003.
66. Gainotti G (2007) Different patterns of famous people recognition disorders in patients with right and left anterior temporal lesions: A systematic review. *Neuropsychologia* 45(8):1591–1607.
67. Talairach J, Bancaud J (1973) Stereotaxic approach to epilepsy: Methodology of anatomo-functional stereotactic investigations. *Prog Neurol Surg* 5:297–354.
68. Benton AL, Sivan AB, Hamsher K, Varney NR, Spreen O (1983) *Benton Facial Recognition: Stimulus and Multiple Choice Pictures* (Psychological Assessment Resources, Lutz, FL).
69. Liu-Shuang J, Norcia AM, Rossion B (2014) An objective index of individual face discrimination in the right occipito-temporal cortex by means of fast periodic oddball stimulation. *Neuropsychologia* 52:57–72.
70. Dzhelyova M, Rossion B (2014) Supra-additive contribution of shape and surface information to individual face discrimination as revealed by fast periodic visual stimulation. *J Vis* 14(14):15.
71. Appelbaum LG, Wade AR, Vildavski VY, Pettet MW, Norcia AM (2006) Cue-invariant networks for figure and background processing in human visual cortex. *J Neurosci* 26(45):11695–11708.

Supporting Information

Jonas et al. 10.1073/pnas.1522033113

SI Text

Statistical Comparison Between Regions. Amplitudes of general visual and face-selective responses were statistically compared across pairs of regions containing groups of face-selective contacts by using a permutation test. Specifically, the signal amplitudes measured at all recording contacts in two given regions were randomly assigned in two bins, with the number of contacts in each bin being equal to the number of contacts in each region. Next, the difference between the means of the two random bins was computed and stored. Because permutation shuffles the region label of each contact, the difference between the means of the two new bins reflects the difference between regions under the null hypothesis (i.e., that the contacts in the two regions are drawn from the same population). This process was repeated 20,000 times to obtain a distribution of differences across regions expected under the null hypothesis. A two-tailed P value was computed as the fraction of the permutation distribution that was either smaller or larger than the observed mean difference between compared regions (depending on the sign of this difference). The minimal attainable P value was constrained by the number of permutations performed (i.e., here, minimal P value = 2/20,000 = 0.0001).

Complementary Analysis with Artifact Rejection. In addition to the analyses reported in the main text, an amplitude quantification analysis after a step of SEEG artifact rejection was performed. For each patient's data, the following steps were performed: the 63-s sequences were segmented in epochs of duration of one cycle of 1.2 Hz (i.e., 833 ms); epochs from separate sequences were pooled together; epochs in which signal amplitude at any time point was above or below 4.5 times the across-epoch SD were rejected (the mean percentage of rejected epochs across participants was 28.8% ± 12.5%); remaining epochs were averaged together; and a FFT was performed on these averaged epochs (frequency resolution of 1.2 Hz). The face-selective and general visual responses at the face-selective contacts identified by our main analysis were quantified by using the same methodology.

Clustered Spatial Organization in Face-Selective Regions. The spatial organization of face-selective responses was explored at a finer scale within the different face-selective regions.

Clustering of face-selective contacts. The tendency of face-selective contacts to be spatially contiguous with each other was determined by measuring for each main region (*i*) the mean distance between face-selective contacts and (*ii*) the mean number of face-selective contacts spatially grouped together (i.e., immediately adjacent to each other). Given that recording contacts are regularly spaced apart on electrodes (i.e., arrays of 8–15 recording contacts), this analysis was performed at the level of individual electrodes in each participant's native anatomy. For each participant, we first selected all VOTC electrodes that contained at least one face-selective contact. Each selected electrode was labeled according to the main region where it was located (OCC, PTL, or ATL). Next, the following steps were performed: (*i*) in each electrode, the number of face-selective contacts contiguously located and the distance between adjacent face-selective contacts were computed and stored; and (*ii*) these values were averaged across participants/electrodes for each main region. The spatial contiguity and mean distances across face-selective contacts were statistically tested by running a randomization test. Specifically, distributions of contiguity and mean distances expected by chance were built by repeating steps (*i*) and (*ii*) 2,000 times after randomly shuffling the location of all contacts from each electrode at each iteration. The significance of the original contiguity and distances were determined by comparing them to the random distribution.

Clustering of highly face-selective contacts. The tendency of the contacts showing the largest face-selective amplitude to be spatially contiguous was also tested. Highly face-selective contacts were defined at the level of single electrodes, as contacts with a distinctively high amplitude relative to the distribution of amplitudes in the electrode. Highly face-selective contacts were identified as contacts with an amplitude >3 SDs from the mean amplitude of the 75% of the contacts with the lowest amplitude. Each electrode was labeled according to the anatomical location of its most face-selective contact (i.e., contact showing the largest face-selective response amplitude). The clustering of highly face-selective contacts in each anatomical region was examined by first determining the proportion of electrodes containing highly face-selective contacts. Among these electrodes, the mean distances between highly face-selective contacts were measured and statistically tested by using a randomization test similar to that described above.

The spatial clustering of face selectivity was further examined in each anatomical region. To do so, the spatial variation of face-selective response amplitude across the length of each electrode (an electrode is an array of recording contacts) was quantified in the following way: (*i*) All VOTC electrodes with at least one face-selective recording contact were selected; (*ii*) the amplitude of the face-selective response at all contacts (face selective or not) of the selected electrodes (i.e., 8–15 contacts separated by 3.5 mm center-to-center, per electrode) was measured; (*iii*) each electrode was labeled according to the anatomical location of its most face-selective contact; (*iv*) all electrodes were spatially aligned with respect to the location of the contact with maximal face-selective response amplitude; (*v*) electrodes were pooled by regions across the left and right hemispheres (to increase the number of data points); (*vi*) each electrode was "folded" around the maximum by averaging amplitude values from equidistant contacts on both sides of the maximum; and (*vii*) the resulting face-selective profiles for each region were averaged. The averaged profiles represent the mean variation of face-selective response amplitude as a function of the distance from the maximum. To statistically assess the clustering of highly face-selective responses in each region, a randomization analysis was used. Specifically, the original averaged face-selectivity profiles was compared with a random distribution of profiles generated by repeating steps (*iv*) to (*vii*) 2,000 times, randomly shuffling the location of contacts separately in each electrode, at each iteration. This process allowed generating for each region a confidence interval for the average profile expected by chance if the contacts were randomly located. Because we centered each electrode relative to the maximum face-selective amplitude both for the original and the random contact locations, both types of profiles exhibit a maximum of equal amplitude. However, if the largest face-selective responses tend to spatially cluster in a given region (and therefore tend to be contiguous to the maximum), the responses around the maximum should be significantly above the profiles computed after randomly shuffling contacts location.

Control Experiment at 1.5-Hz Stimulation Rate. To ensure that the pattern of variation of the general visual responses across regions was independent from the stimulation rate (6 Hz), the amplitude of general visual responses was measured in an additional control experiment performed in 11 of our participants. They performed the exact same experiment but with a lower base frequency rate (base frequency, 1.5 Hz; face-selective frequency, 1.5/5 = 0.3 Hz;

three to six sequences of 70 s per participant). General visual responses at 1.5 Hz were quantified at each face-selective contact (defined using the 6-Hz experiment) as the sum of the baseline-corrected amplitude across harmonics (up to the highest significant harmonic across patients, i.e., 24 Hz for the 6-Hz experiment and up to 13.5 Hz for the 1.5-Hz experiment).

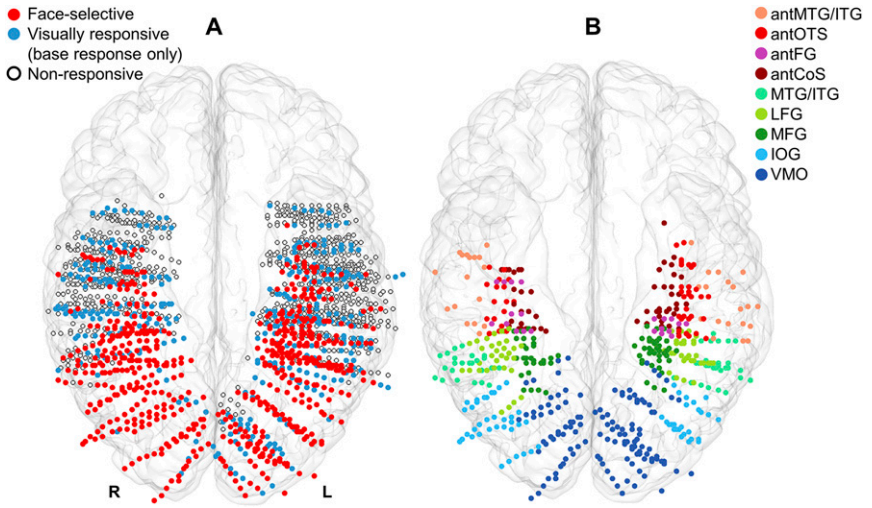

Fig. S1. Spatial distribution of face-selective, visually responsive, and nonresponsive contacts in the MNI space (ventral view). (*A*) Map of all 1,678 VOTC recording contacts across the group of 28 participants displayed in the MNI space using a transparent reconstructed cortical surface of the Colin27 brain. Each circle represents a single contact. Face-selective contacts (red) are represented along with contacts visually responsive to the base frequency but not face-selective (blue) and nonresponsive contacts (white, no face-selective or general visual responses recorded). The number of recorded contacts was higher in the left than in the right hemisphere (988 vs. 690). (*B*) Face-selective contacts in the MNI space colored according to their anatomical label in the individual anatomy.

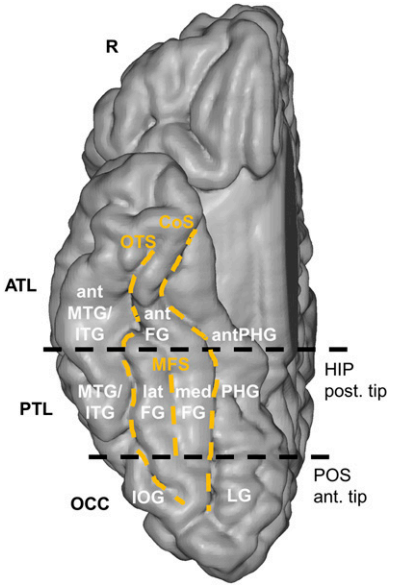

Fig. S2. Schematic representation of the parcellation scheme used to determine the anatomical label of each face-selective contact. Anatomical regions were defined in each individual hemisphere according to major anatomical landmarks. The ventral temporal sulci [CoS, OTS, and midfusiform sulcus (MFS)] serve as medial/lateral borders of regions, whereas two coronal reference planes containing anatomical landmarks [posterior tip of the HIP and anterior tip of the parieto-occipital sulcus (POS)] serve as an anterior/posterior boundary for each region. The anatomical location of each face-selective contact was determined in the individual brain according to this anatomical subdivision and contacts were grouped by anatomical location across all participants. The schematic locations of these anatomical structures are shown on a reconstructed cortical surface of the Colin27 brain.

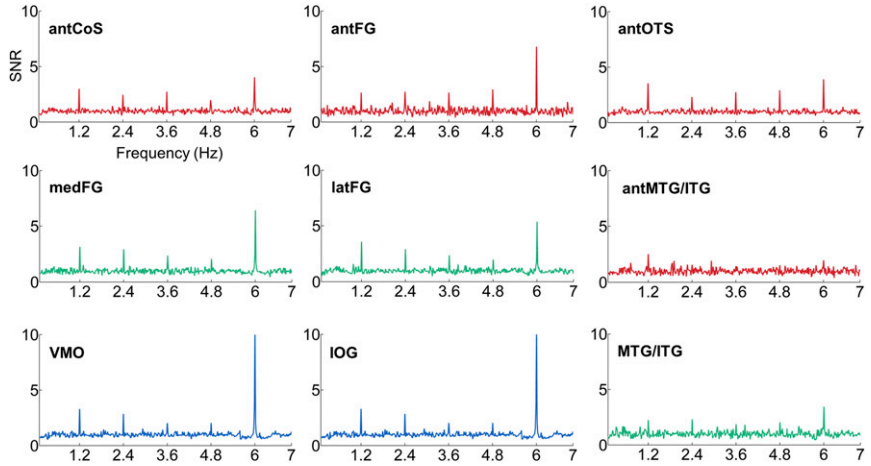

Fig. S3. Averaged iEEG frequency spectra in each region of the left hemisphere. IEEG frequency spectra in each region of the left hemisphere averaged across all face-selective contacts located in the same region are shown.

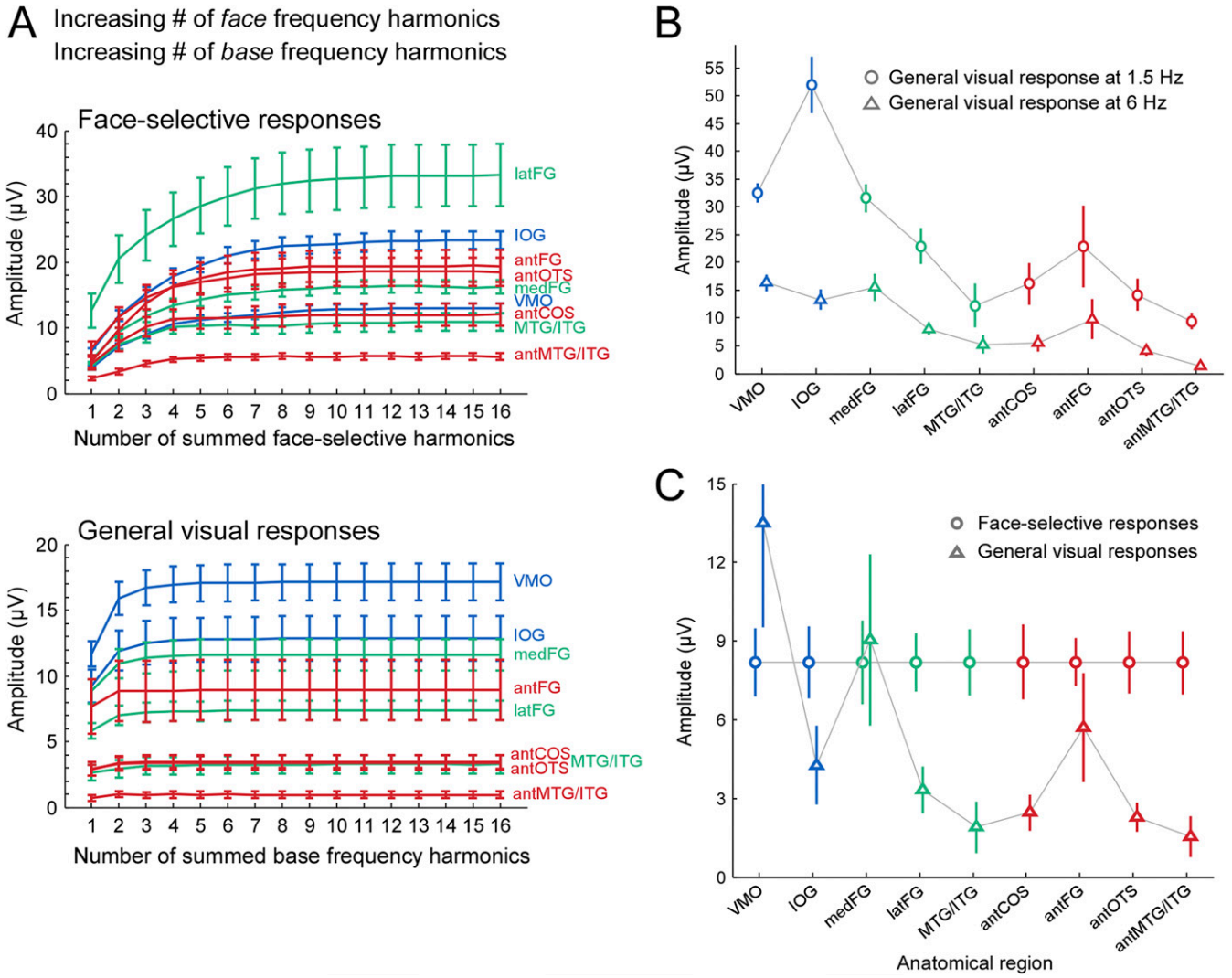

Fig. S4. Control analyses and experiments. (*A*) The pattern of response amplitudes is independent from the number of harmonics included in the quantification. Although the number of harmonics included to quantify the responses was objectively defined (from the first until the highest significant harmonic across participants), the pattern of results is stable whatever the number of harmonics included in the analyses. Here face-selective responses (*Upper*) and general visual responses (*Lower*) are quantified as a function of the number of harmonics included in the analyses. Data are represented as the mean across contacts for each VOTC region (SEMs across contacts are represented as error bars). Differences between regions already emerge from the first harmonics and remain stable regardless of the number of face or base frequency harmonics used in the analyses. (*B*) The decrease of the general visual response in anterior regions does not result from an inability of these anterior regions to generate a response at 6 Hz. The figure compares the mean baseline-subtracted amplitude of general visual responses in the 1.5-Hz experiment (control experiment) to the general visual responses in the 6-Hz experiment (main experiment) in the 11 patients who performed both experiments. The same pattern of response amplitude in the 6- and 1.5-Hz base rate experiments are found, with a decrease of amplitudes from posterior to anterior regions. (*C*) The decrease of the general visual response in anterior regions is not due to a global response amplitude reduction. The mean baseline-subtracted amplitude of the general visual responses is compared across regions for groups of contacts showing similar mean face-selective response amplitudes. To do so, the following analysis was performed: (*i*) contacts from left and right regions were grouped together; (*ii*) in each region, contacts for which the face-selective response amplitude was located between 0 and 15 μV were selected (based on the range of the response of the least responsive region: antMTG/ITG): the minimum number of contacts within this amplitude range across regions was 7 in antFG; (*iii*) for each region a combination of 7 contacts (by randomly sampling from the pool of contacts in the range of 0–15 μV) for which the mean amplitude was the closest to the mean amplitude of the region with the least number of contacts (i.e., antFG: 7 contacts) was searched for; and (*iv*) the mean general visual response amplitude at corresponding contacts was extracted. A similar reduction of general visual responses from posterior to anterior regions as for the main analysis with all of the contacts was observed.

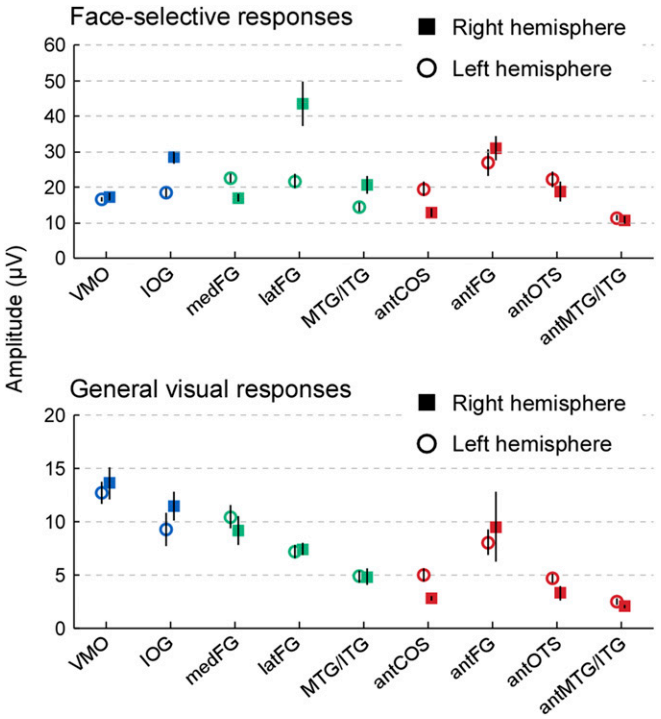

Fig. S5. Quantification of mean face-selective and general visual responses in each region after artifact rejection. The average across contacts for each region is shown separately for the left and right hemispheres. Error bars represent the SEM across contacts. For the artifact rejection procedure, see *SI Text*.

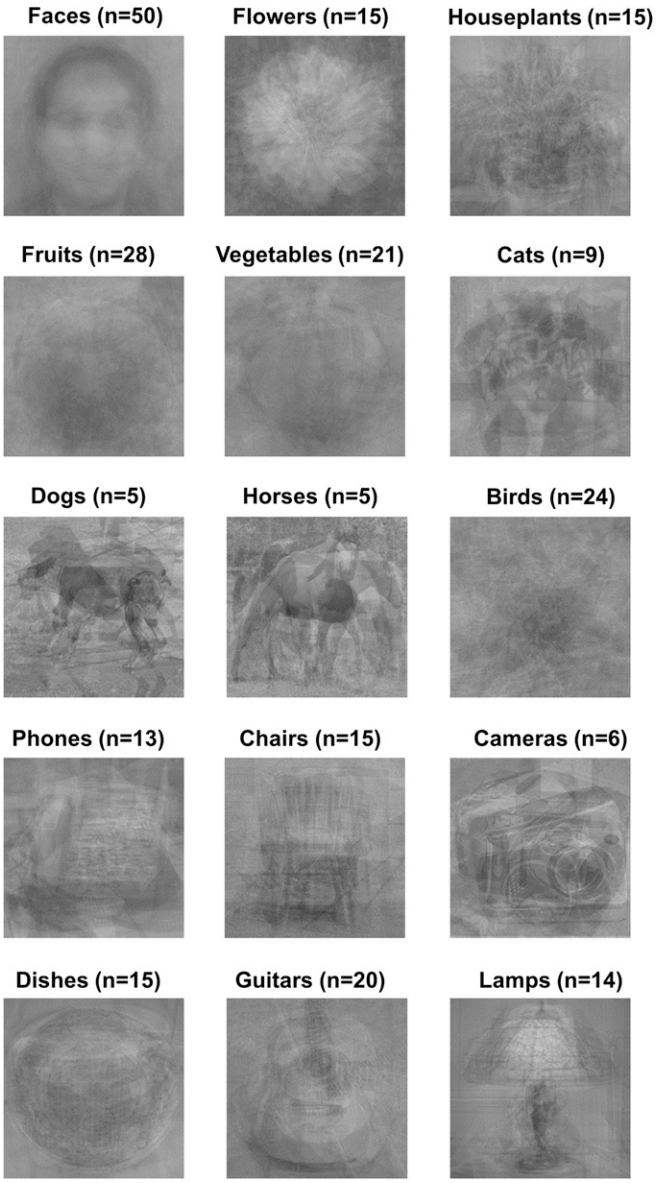

Fig. S6. Average across images in each category (faces and 14 categories including cats, dogs, horses, birds, flowers, fruits, vegetables, houseplants, phones, chairs, cameras, dishes, guitars, and lamps). *n* indicates the number of images for each category in our set of stimuli.

Table S1. Talairach and MNI coordinates of each region

	Left			Right		
Regions	*x*	*y*	*z*	*x*	*y*	*z*
Talairach						
VMO	−16 ± 9	−80 ± 12	3 ± 13	18 ± 7	−75 ± 12	1 ± 7
lOG	−37 ± 6	−74 ± 6	−8 ± 6	43 ± 9	−71 ± 8	−7 ±10
medFG	−24 ± 4	−44 ± 6	−11 ± 4	28 ± 5	−46 ± 6	−10 ± 6
latFG	−38 ± 6	−46 ± 5	−12 ± 4	41 ± 6	−45 ± 7	−16 ± 6
MTG/ITG	−48 ± 6	−50 ± 7	−9 ± 8	55 ± 7	−48 ± 4	−9 ± 9
antCoS	−29 ± 5	−23 ± 10	−17 ± 6	32 ± 6	−23 ± 9	−15 ± 7
antFG	−28 ± 3	−31 ± 5	−18 ± 1	35 ± 6	−24 ± 8	−23 ± 4
antOTS	−38 ± 3	−23 ± 11	−20 ± 5	40 ± 4	−21 ± 9	−20 ± 7
antMTG/ITG	−55 ± 9	−26 ± 12	−15 ± 5	55 ± 5	−16 ± 11	−16 ± 4
MNI						
VMO	−15 ± 8	−80 ± 12	2 ± 12	17 ± 7	−77 ± 13	1 ± 7
lOG	−36 ± 6	−75 ± 6	−7 ± 6	42 ± 9	−75 ± 9	−7 ± 9
medFG	−24 ± 4	−46 ± 6	−11 ± 4	26 ± 5	−49 ± 7	−9 ± 5
latFG	−36 ± 5	−48 ± 5	−12 ± 3	41 ± 6	−49 ± 9	−16 ± 5
MTG/ITG	−48 ± 7	−53 ± 6	−9 ± 7	53 ± 7	−52 ± 5	−9 ± 9
antCoS	−28 ± 4	−25 ± 10	−16 ± 6	31 ± 5	−27 ± 10	−15 ± 6
antFG	−28 ± 4	−36 ± 3	−17 ± 1	35 ± 5	−29 ± 9	−21 ± 4
antOTS	−37 ± 3	−25 ± 11	−20 ± 5	40 ± 3	−26 ± 9	−20 ± 6
antMTG/ITG	−52 ± 8	−27 ± 11	−14 ± 5	52 ± 6	−19 ± 13	−16 ± 4

Values are mean coordinates of face-selective contacts ± SD.

Table S2. Regions of interest ranked from the highest to the lowest face-selective response amplitude, and the corresponding general visual response amplitude

Regions	Hemisphere	Mean face-selective response (μV)	Mean general visual response (μV)
LFG	Right	45.47 ± 8.0	7.02 ± 0.9
lOG	Right	25.11 ± 1.6	12.03 ± 1.9
antFG	Right	22.28 ± 3.3	9.99 ± 4.3
lOG	Left	20.62 ± 2.3	13.59 ± 3.1
antOTS	Left	19.80 ± 2.9	3.93 ± 0.6
latFG	Left	19.44 ± 3.0	7.55 ± 1.2
medFG	Left	18.30 ± 1.5	11.69 ± 1.6
antFG	Left	16.13 ± 3.4	7.65 ± 1.4
antOTS	Right	15.90 ± 3.0	2.44 ± 0.8
antCoS	Left	13.97 ± 2.6	4.19 ± 0.9
medFG	Right	13.63 ± 1.1	11.26 ± 1.8
VMO	Left	13.27 ± 1.0	17.58 ± 1.8
MTG/ITG	Right	12.62 ± 2.5	2.16 ± 1.1
VMO	Right	12.34 ± 0.8	15.86 ± 2.0
MTG/ITG	Left	9.20 ± 1.2	3.99 ± 0.8
antCoS	Right	9.04 ± 1.6	2.23 ± 0.3
antMTG/ITG	Right	5.74 ± 0.8	0.94 ± 0.2
antMTG/ITG	Left	5.62 ± 0.6	0.99 ± 0.4

Values are means ± SE.

Movie S1. Sample movie of the fast periodic sequence.

Movie S1